Catalysis Today 141 (2009) 300–305

Contents lists available at ScienceDirect

Catalysis Today

journal homepage: www.elsevier.com/locate/cattod

Interaction of vanadium containing catalysts with microwaves and their activation in oxidative dehydrogenation of ethane

Ilia Sinev [a,*], Tatiana Kardash [b], Natalia Kramareva [a], Mikhail Sinev [c], Olga Tkachenko [a], Alexei Kucherov [a], Leonid M. Kustov [a]

[a] Zelinsky Institute of Organic Chemistry, R.A.S., Moscow 119991, Russia
[b] Boreskov Institute of Catalysis, Novosibirsk 630090, Russia
[c] Semenov Institute of Chemical Physics, R.A.S., Moscow 119991, Russia

ARTICLE INFO

Article history:
Available online 16 June 2008

Keywords:
Catalyst
Microwave activation
Dehydrogenation
Ethane
Molybdenum
Vanadium
Niobium
Antimony

ABSTRACT

Microwave (MW)-activated oxidative dehydrogenation of ethane is studied using kinetic approach. It consists in the comparison of kinetic dependencies (shape of kinetic equations, "selectivity or yield vs. conversion" curves) and apparent parameters (activation energies) obtained in thermal and MW modes. In the case of VMo and VMoNb oxides a distinct difference between ethane yields was observed at given conversion of limiting reactant (oxygen). It was proven by X-ray diffraction that MW activation changes the catalyst microstructure forming phase distribution different from that formed under a conventional heating and thus changing catalytic behavior of VMo and VMoNb oxides.

1. Introduction

Being the major components of petroleum gas, C_2–C_4 alkanes can serve as raw materials in the production of a variety of petrochemical products being first converted into corresponding olefins. Unfortunately, due to a relatively low chemical activity of light alkanes (LA), only a limited fraction of their total production undergoes chemical processing. Substantial amounts of LA are burned in gas flares or released to atmosphere. As a result, concentration of greenhouse gases in atmosphere is increasing simultaneously with an irreversible loss of potentially valuable chemical raw materials. The best way to avoid this mindless waste of hydrocarbon resources is to convert them into high value-added products (including bulk chemicals, motor fuels, etc.). Oxidative dehydrogenation (ODH) of light alkanes to corresponding olefins can be the first step of such conversion.

The ODH process is not only important from an industrial standpoint and its possible contribution to the well-being of modern mankind. As the simplest process of partial oxidation of light alkanes, it also presents the opportunity for a fundamental research aimed at an understanding of catalytic behavior on molecular level and forming a basis for rational design of improved catalysts for existing processes and the discovery of totally new catalysts and technologies.

The processes of non-oxidative dehydrogenation (NOD) of LA (e.g., ethane and propane) to corresponding olefins are commercially well established. Among commercialized, the best known are Star (Philips Petroleum), Catofin (Lummus), Oleflex (UOP), Linde-BASF and Snamprogetti–Yarsintez processes. The main disadvantages of the whole family of NOD processes are their thermodynamically limited olefin yields, high energy input required to compensate their inherent endothermicity, high rate of coke formation and, as a result, a low durability of the catalysts used.

The ODH process is free of the above disadvantages. Moreover, it can be a net producer of energy (due to the exothermicity of the ODH reaction itself and to the additional heat evolution in a parallel and/or sequential total oxidation). However, due to a much higher reactivity of target products (olefins) compared to the initial LA's, ODH selectivity drastically drops at increasing conversion, and all catalysts existing to date suffer from a limited selectivity to olefins, especially in the case of C_{3+} alkanes. Thus, further development of industrially viable ODH process depends on the progress in the catalyst design based on a deeper understanding of catalytic action.

* Corresponding author at: Zelinsky Institute of Organic Chemistry, R.A.S., Leninsky Prospect 47, Moscow 119991, Russia. Fax: +7 49513 72935.
E-mail addresses: sinevi@gmail.com, sinevi@aport2000.ru, samorodok@hotbox.ru (I. Sinev).

0920-5861/$ – see front matter © 2008 Elsevier B.V. All rights reserved.
doi:10.1016/j.cattod.2008.04.021

On the other hand, the production of target products can be improved by using some approaches to activation of catalyst(s) and/or catalytic processes different from a conventional thermal heating. Among other physical methods, which provide such non-thermal activation of catalyst, the use of microwave (MW) radiation has evolved over the past two decades. Under microwave irradiation, the electric field induces additional motions of ionic species and polar molecules around their equilibrium positions in the solid. The local heat, which is generated by such microscopic motions, is fundamentally different from classical thermal heating in which energy is uniformly supplied to all atoms present in the structure [1]. Such a non-uniform heating of the catalyst can cause non-conventional product distributions, especially in the case of multi-functional catalysts and complex multi-step reaction if different steps of the latter proceed on different elements of the catalyst structure.

Furthermore, the consideration of the macroscopic behavior of the reactor shows, that microwave energy can be directly delivered to the catalyst without heating the surroundings. Taking into account that gas-phase reactions in a void volume of the reactor can contribute to LA oxidation, it is reasonable to assume that the net result of the MW irradiation of the reaction system can differ from the one accessible under a conventional thermal heating.

The MW effect upon the catalysts could differ depending on their nature. Being microwave-transparent, most of oxide catalyst supports (zeolites, Al_2O_3, MgO and SiO_2) do not absorb MW power and remain relatively cold under the irradiation. As to the temperature of metal particles supported on such materials is determined by the competition between the MW absorption and the energy conversion/dissipation rates. Wan [2] and co-workers mixed microwave-absorbing ferromagnetic and paramagnetic metal catalysts with microwave-transparent solvents. They found that pulsed MW irradiation improves temperature control because the excessive reaction heat can dissipate through the microwave-transparent matrix during the dead cycle time in the course of the pulsed operation. Secondary reactions can thus be minimized due to lower gas-phase and catalyst bed temperatures. Mingos and Zhang [3] explained their results obtained in the decomposition of H_2S over γ-Al_2O_3 supported metal sulfides by a significant apparent shift in the equilibrium constant due to the development of hot-spots in the catalytic beds. The comparison of X-ray diffraction patterns demonstrated some important differences between the catalyst samples obtained by MW treatment and in a conventional thermal mode.

The above-mentioned effects caused by a non-uniform heating of different zones of the catalyst and/or in the catalyst bed are usually considered as "thermal" MW effects. Besides them, some non-thermal effects related to the formation of structures, which cannot be reached under conventional activation, may take place under stress caused by the MW irradiation. Such structural changes may affect catalytic properties in the course of MW activation. Roussy et al. [4] discusses the behavior of $BaBiO_{3-x}$ catalyst in the conditions of oxidative coupling of methane in different modes of activation. The increase of selectivity in the microwave field is attributed to a decrease in the formation of surface oxygen which causes a different behavior of the catalyst as opposed to the conventional heating. Such difference in the behavior of the material was proven by measurements of real and imaginary components of dielectric constant in the microwave field. The latter were performed in monomode at a high microwave energy input for heating of the catalyst, and in a classic resonator (broadband permittivity measurements [5] with low microwave energy input after thermal heating of the sample to a given temperature).

In this paper we present the results of the study aimed at the revealing the effect of MW upon the structure and catalytic performance of several V-containing mixed oxides previously reported in literature as efficient catalysts for oxidative dehydrogenation of LA (see, for instance, Refs. [6,7]). The analysis of kinetic features and parameters obtained in two modes (MW and conventional "thermal") was used to reveal the peculiar effects of *in situ* MW irradiation.

As it was mentioned earlier, some authors assume that the formation of superheated areas in microwave-activated catalysts is taking place. Unfortunately, most of powerful physicochemical methods for studying the catalyst structure are inaccessible during MW activation. Moreover, an experimental isolation of such areas, as well as a direct measurement of their local temperature in MW mode is hardly accessible. As a result, the comparison of data obtained in two modes by plotting "conversion/selectivity/yield vs. temperature" curves could lead to substantial errors in the analysis and conclusions. To overcome this problem, a different – kinetic – approach was used to distinguish between thermal and non-thermal effects of microwave irradiation. It consists in the comparison of apparent kinetic dependencies (shape of kinetic curves, "*S* or *Y* vs. *X*" functions) and parameters (kinetic orders, activation energies) obtained in different modes of activation.

2. Experimental

2.1. Catalyst preparation

2.1.1. $VMoNbO_x$

Ammonium metavanadate NH_4VO_3 (0.562 g) and ammonium paramolybdate (3.383 g) were dissolved in saturated aqueous solution of oxalic acid (200 ml) while stirring at 70 °C; after 30 min five drops of hydrogen peroxide were added to resulting suspension and the mixture was stirred until the formation of bright-green transparent solution. Then 1.044 g of niobium oxalate (with Nb_2O_5 content 0.335 g) was added and stirred until dissolution. The residue formed after the evaporation of this solution for 7 h at 100 °C was milled in agate mortar and decomposed at melting while heating to 180 °C with permanent stirring. The residue of black color was twice calcined at 400 °C for 5 h with intermediate grinding. The atomic ratio of metal components in the final mixed oxide is V:Mo:Nb = 1:4.3:0.6.

2.1.2. $VMoO_x$

This sample was prepared using similar procedure without adding the niobium salt. The final calcination temperature in this case was 500 °C. The atomic ratio of metal components in the final mixed oxide is V:Mo = 1:4.

2.1.3. $VSb_{0.1}O_x$

Bulk and supported $VSbO_x$ (V/Sb = 8.8) catalysts were prepared by the citrate method using ammonium monovanadate (Merck) and antimony chloride (Aldrich) as starting materials. Appropriate amounts of NH_4VO_3 and $SbCl_3$ were dissolved in water at heating; in the case of $SbCl_3$, hydrochloric acid was added to suppress its hydrolysis. Transparent solutions were cooled down to ambient temperature and kept for 5 min under ultrasonic treatment. Then citric acid ($C_6H_8O_7{\cdot}H_2O$, Merck) aqueous solution was added to each solution (1.1 equiv.g of acid function per valence-gram of a metal). Thus obtained solutions were agitated for 1 h, then mixed and stirred for 8 h. The mixture was evaporated in Rotavapor at 40 °C under reduced pressure to from a syrup-like liquid, and then dried in a vacuum oven at 80 °C for 24 h. Thus obtained solid precursor was decomposed at 300 °C for 16 h and calcinated at 550 °C for 8 h in air. The final solid was used as a bulk catalyst. To

prepare the supported catalyst with the same ratio of active components (V and Sb), a microspheric θ-Al_2O_3 (MNTK "Katalizator", ~85 m^2/g) was impregnated with mixed V–Sb–citrate solution during 2 h at room temperature; all subsequent operations were the same as described for the bulk catalyst. The supported component loading was 17.7 wt.%.

2.2. Catalytic activity tests

Catalytic tests were performed under atmospheric pressure in a continuous gas flow system. The straight down-flow tubular quartz microreactor (internal diameter 7 mm) with a fixed catalyst bed was used. Reactor with catalyst (0.4 g loading, particle size 0.2–0.5 mm) was heated either by electric resistance furnace, or by MW irradiation. The temperature in the catalyst bed in both MW and thermal modes was monitored by an optical fiber thermal sensor in a thermo-wall placed in the center of the bed. A reaction mixture containing 33.6 vol.% ethane and 16.8 vol.% oxygen in N_2 was fed into the reactor by mass-flow controller at a total flow rate ranging from 10 to 90 cm^3/min. Reactants and products were analyzed by an on-line gas chromatograph equipped with thermal conductivity detector and two parallel stainless steel columns packed with Porapack-Q (2 m) for separation of CO_2, ethylene, ethane; CaA molecular sieves (2 m) for separation of permanent gases (O_2, N_2 and CO). Helium was used as a carrier gas.

Catalytic behavior was characterized by total conversion of reactants ($X_{C_2H_6}, X_{O_2}$), selectivity of ethylene formation (S) and yield (Y) of ethylene: $Y = X_{C_2H_6} \times S$.

2.3. Microwave apparatus

Microwave activation was studied using a specially designed low-power microwave reaction system (Fig. 1). The reactor with catalyst was inserted into the microwave cavity irradiated by a magnetron-based MW generator operated in continuous regime at frequencies ranging from 3.4 to 3.8 GHz. The cavity was designed to focus the maximum of microwave power in its center where the catalyst bed was positioned. The incident power varied from 10 to 50 W was delivered to the microwave cavity (1) via coaxial waveguide (2). Incident and reflected power were measured with wattmeters (3 and 4), respectively.

2.4. X-ray diffraction (XRD)

Powder XRD patterns were recorded with a DRON 3M diffractometer with Cu Kα1 radiation in Bragg–Brentano reflecting and Debye–Sherrer transmission geometry (λ = 1.54 Å).

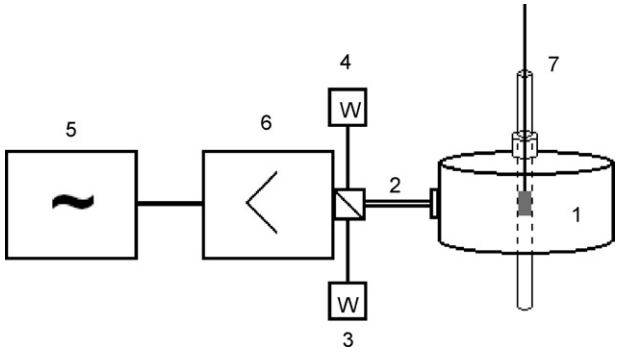

Fig. 1. Microwave apparatus for *in situ* catalyst activation: 1—microwave cavity (resonator); 2—coaxial waveguide; 3 and 4—wattmeters; 5—microwave generator; 6—broadband amplifier; 7—quartz reactor with thermo-wall.

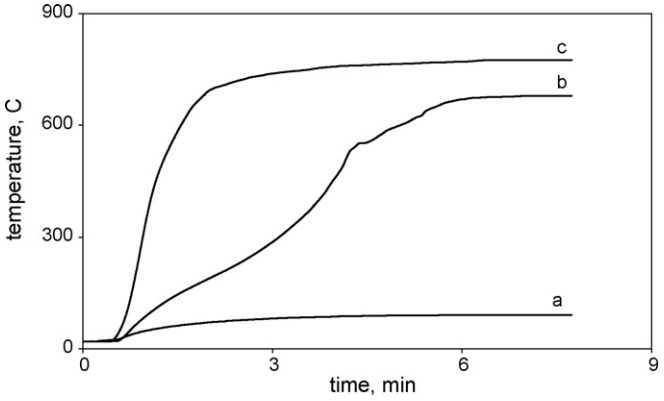

Fig. 2. Catalysts heating curves during MW activation: a—$VSbO_x/\gamma$-Al_2O_3; b—$VMoNbO_x$; c—$VSbO_x$.

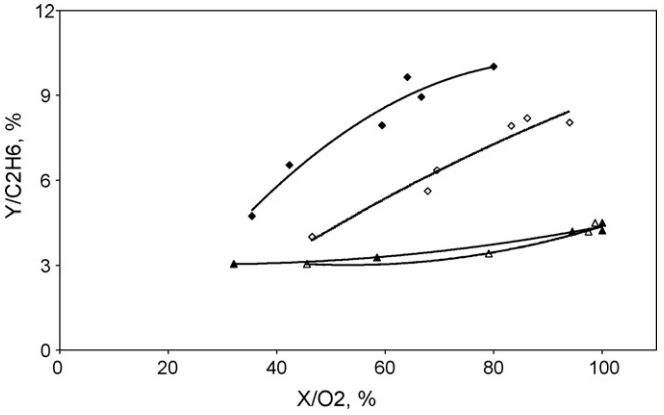

Fig. 3. Ethylene yield as a function of oxygen conversion in thermal and MW modes: $VSbO_x$ microwave (▲) and thermal (△) activated and $VMoNbO_x$ microwave (◆) and thermal (◇) activated.

2.5. X-ray photoelectron spectroscopy (XPS)

X-ray photoelectron spectra were obtained using an XSAM-800 spectrometer with Mg Kα radiation for spectra excitation. The values of electron binding energies were corrected taking into account sample charging using the C 1s peak at 285.0 eV as a reference. The atomic concentration was calculated from the

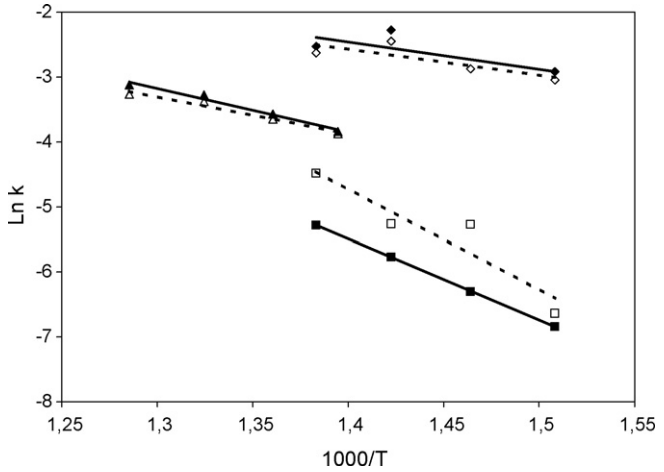

Fig. 4. Arrhenius plots (K—overall ethane conversion apparent rate constant): $VSbO_x$ microwave (▲) and thermal (△) activated; $VMoNbO_x$ microwave (◆) and thermal (◇) activated; $VMoO_x$ microwave (■) and thermal (□) activated.

integral intensity of XPS peaks using the Scoefild photoionization cross-sectional data [8].

3. Results and discussion

3.1. Interaction of samples with microwaves

Fig. 2 demonstrates thermal effects arising from catalyst interaction with MW-irradiation. Curves represent heating of $VMo(Nb)O_x$ (curve *b*) and bulk (curve *a*) and supported (curve *c*) $VSbO_x$ at the maximum available power. Evidently, bulk catalysts actively absorb the MW radiation, which results in their heating to typical ethane ODH temperatures (400–500 °C). In the case of supported $VSbO_x$ the maximum accessible temperature does not exceed 150 °C. The major constituent of this sample – alumina support – is transparent for microwaves and remains unheated while irradiated. Subsequent catalytic experiments revealed that the supported active $VSbO_x$-component also does not reach the temperature required for ODH reaction.

As can be seen from Fig. 2, the heating curves of $VMo(Nb)O_x$ samples consist of several segments. These features can be attributed to phase transitions and/or structure changes in these

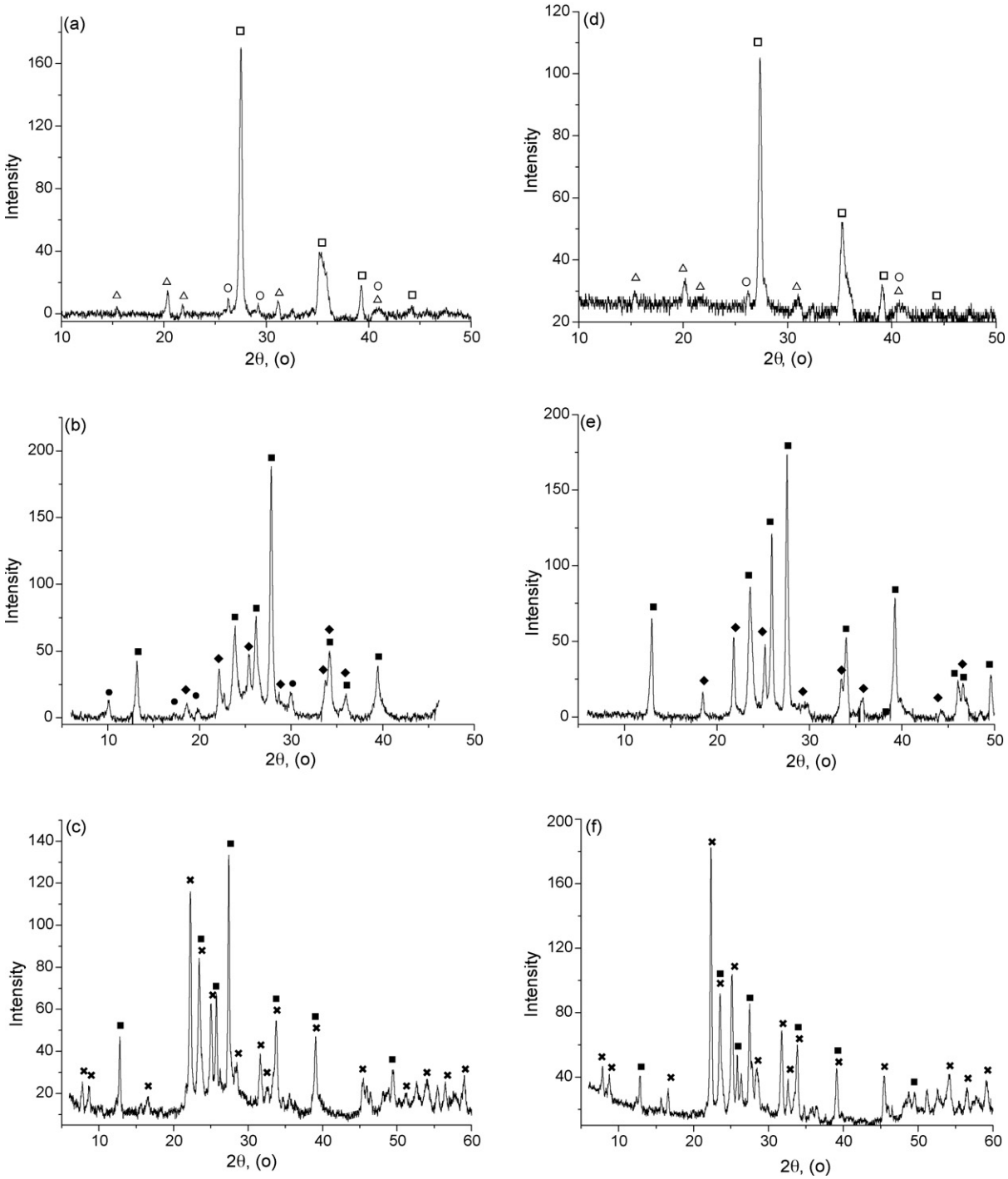

Fig. 5. X-ray diffraction of $VSbO_x$ (a—microwaved; d—thermally heated), $VMoO_x$ (b and e) and $VMoNbO_x$ (c and f). Symbols: $(SbV)O_4$ (□); V_2O_5 (△); SbO_4 (○); MoO_3 (■); V_2MoO_8(▲); $(NH_4)_xV_xMo_{1-x}O_3$ (●); θ-$(Mo_{1-x}Me_x)O_{2.8}$ (×).

samples appeared under the MW irradiation. Such changes leading to variations of physical properties of the oxide bulk lead, in turn, to corresponding changes in the ability to interact with electromagnetic field and, as a result, to changing heating rate under the MW irradiation. The most unexpected results were obtained while heating the VMo(Nb)-oxides: absorption of MW power is accompanied by the appearance of catalyst grains with the color changed from dark green to orange evidencing for a deep oxidation of constituent cations (in particular, vanadium transition to V^{5+} state). The latter cannot be reached by regular thermal oxidation of this sample in air at any temperature. It is worth noticing that this unusual state of the oxide is not stable (or it is metastable): such orange coloring disappears while standing at room temperature within several hours; this "relaxation" is accelerated by moderate heating and grinding in mortar. Evidently, the processes which lead to the formation of orange-colored areas in VMo(Nb) oxides cannot be explained by different heating of different elements of their structure, but are likely to have a more complex nature.

3.2. Catalytic performance in thermal and MW modes

Catalytic experiments demonstrate that catalysts under study are active in ethane ODH. Also, in the case of bulk oxides, distinct differences in their kinetic behavior were observed depending on the activation mode.

The analysis of "conversion vs. reciprocal flow rate (residence time)" curves demonstrated that in both modes of operation the overall rate can be satisfactorily described by a simple first-order equation (straight lines on "$\mathrm{Ln}(1-X)$ vs. W^{-1}" plots), which allows one to extract from the experimental data pseudo-first order rate constants for each sample and to further analyze them. For instance, in the case of VMo-oxide two Arrhenius plots obtained in different activation modes differ significantly. Corresponding values of apparent activation energies for MW and thermal modes are 124 and 99 kJ/mole. This is an indication that the MW irradiation modifies the properties of active sites responsible for activation of initial reactant molecules.

On the other hand, in the case of VMoNb oxide a distinct difference between ethylene yields is observed at a given conversion of limiting reactant (oxygen) (Fig. 3). Since for the same $VMoNbO_x$ catalyst no significant difference in Arrhenius plots in two modes is noted (see Fig. 4), one may assume that the unusual structures existing in the conditions of MW irradiation contribute to the reaction on the stage of consecutive transformation of reactive intermediate products.

3.3. Catalyst phase composition

The XRD patterns of $VSbO_x$, $VMoO_x$ and $VMoNbO_x$ catalysts activated under the conventional (a–c) and MW heating (d–f) are presented in Fig. 5. It can be seen that patterns a and d do not differ considerably indicating that the effect of microwaves onto a mixed vanadium–antimony oxide can be considered as "thermal" (i.e., the MW irradiation is just another way of heating the sample to the reaction temperature). This is in a good agreement with the data described above that showed no difference in the kinetic features of the ODH reaction over this catalyst in two modes.

Both diffractograms of $VMoO_x$ sample (b and e) exhibit the reflections typical for rhombic MoO_3 [JCPDS 35-609] and V_2MoO_8 [JCPDS 18-0851]. The diffraction patterns of thermally heated $VMoO_x$ though contain reflections similar to $(NH_4)_xV_xMo_{1-x}O_3$ [9] phase, also called hexagonal MoO_3, which forms during preparation if calcintiont temperature is below 500 °C. Alternatively, these reflections could be associated with paramolybdate precursor. After the MW treatment of $VMoO_x$ the reflexes attributed to hexagonal type MoO_3 phase disappear; the degree of crystallinity of V_2MoO_8 phase increases.

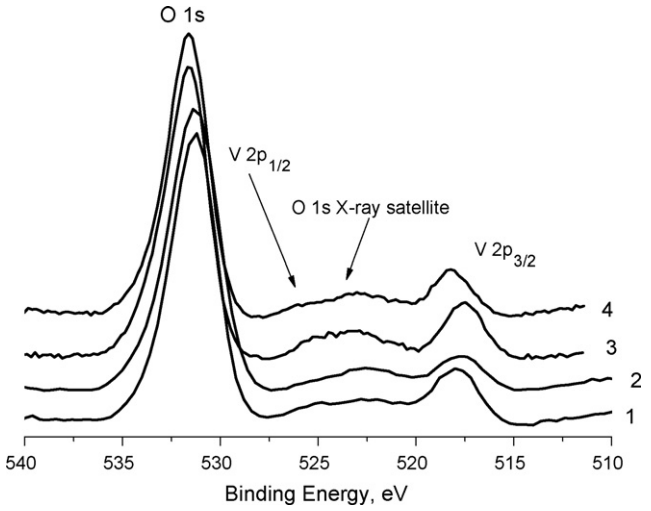

Fig. 6. X-ray photoelectron spectra of O 1s + V 2p region: 1—before catalysis; 2—after catalysis with MW; 3—after conventional catalysis; 4—after MW in air.

$VMoNbO_x$ patterns evidence for the presence of rhombic MoO_3-[JCPDS 35-609] and V- [JCPDS 31-1437] and Nb-substituted [JCPDS 35-1312, 27-1310] θ-molybdenum oxides $(Mo_{1-x}Me_x)O_{2.8}$ with a Mo_5O_{14}-like structure [10]. It can be concluded that in the MW-treated sample the fraction of MoO_3 phase decreases at the expense of Mo_5O_{14}-like structure, which is found to be active component in $VMoNbO_x$ ODH catalysts [10].

3.4. XPS

Typical XPS V 2p spectra together with the nearby O 1s lines are presented in Fig. 6. The XPS results showing the influence of different treatments on the spectra of the fresh mixed oxides (before catalysis) are summarized in Table 1. The position of V $2p_{3/2}$ component shifts to lower binding energies (0.3–0.4 eV) after catalytic reaction in both thermal and MW modes. This small negative shift might indicate a partial reduction of V^{5+} to V^{4+} surface oxide species [11,12]. The B.E. of V $2p_{3/2}$ component demonstrates the increasing electron deficiency on V species after treatment of $VMoO_x$ sample in air under the MW irradiation.

As we mentioned above, the appearance of unusual orange coloring in VMo(Nb) oxides under the MW irradiation can be explained by some changes in the oxidation state of vanadium (its oxidation to the highest oxidation degree V^{5+}) which cannot be reached in a mixed oxide by any thermal treatment. Unfortunately, this effect could not be supported by XPS data because of a metastable character of this unusual state. The orange coloring disappeared during the preparation of the sample to XPS measurements, which includes a grinding in mortar.

No changes in the electronic state of Mo were observed in XPS spectra of mixed oxides after any treatments.

Table 1
XPS binding energy and surface atomic ratio

Sample	Binding energy (eV)			V/Mo
	O 1s	V $2p_{3/2}$	Mo $3d_{5/2}$	
Before catalysis	531.0	517.9	233.3	0.26
After catalysis with MW	531.0	517.6	233.3	0.17
After conventional catalysis	531.6	517.5	233.3	0.34
After MW treatment in air	531.6	518.3	233.3	0.25

The influence of treatments on the component concentration in the surface and subsurface layers of about 3 nm thickness was detected. The increase of V/Mo atomic ratio after the conventional catalytic reaction and the decrease of this value upon the MW irradiation are taking place. The V/Mo ratio after the MW irradiation in air remains constant. These trends are likely to indicate either the re-dispersion or migration of vanadium in the mixed oxide lattice.

4. Conclusion

Structural data and kinetic analysis of ODH reaction over a series of V-containing mixed oxides both demonstrate that microwave irradiation has only a "thermal" type effect on VSb-sample. On the contrary, mixed oxides of V-Mo group undergo changes associated with the formation of modified phase compositions and unusual oxidation states of cations (namely vanadium) which are not accessible under a conventional thermal heating. These structural changes lead to a different catalytic performance, either on the stage of reactant activation (VMo-oxide) or in consecutive transformations of reaction intermediates (VMoNb-oxide).

Acknowledgements

Authors acknowledge the financial support from Haldor Topsoe A/O Company. We also wish to thank Dr. I.V. Mishin for his help in XRD analysis.

References

[1] G. Roussy, et al. J. Microw. Power Electromagn. Energy 22 (1987) 989.
[2] J.K.S. Wan, Res. Chem. Intermed. 19 (1993) 147.
[3] X. Zhang, D.O. Hayard, D.M.P. Mingos, Chem. Commun. (1999) 975.
[4] G. Roussy, E. Marchale, J.M. Thiebaut, A. Kiennemann, Fuel Process. Technol. 50 (1997) 261.
[5] G. Roussy, et al. Meas. Sci. Technol. 12 (2000) 542.
[6] E.A. Mamedov, V. Cortés Corberán, Appl. Catal. A 127 (1995) 1–40.
[7] S. Albonetti, F. Cavani, F. Trifiró, Catal. Rev. 38 (1996) 413–438.
[8] J.H. Scoefild, J. Electron. Spectrosc. 9 (1976) 29.
[9] G.A. Zenkovec, et al. Izvestiya AN USSR Neorganicheskie Materialy 15 (1979) 313 (in Russian).
[10] V.M. Bondareva, T.V. Andrushkevich, G.I. Aleshina, React. Kinet. Catal. Lett. 8 (2006) 377.
[11] G. Ciarello, D. Robba, G. De Michele, F. Parmigiani, Appl. Surf. Sci. 64 (1993) 91.
[12] L.E. Briand, O.P. Tkachenko, M. Guraya, X. Gao, I.E. Wachs, W. Grünert, J. Phys. Chem. B 108 (15) (2004) 4823.